Developmental Biology 446 (2019) 142–150

Contents lists available at ScienceDirect

Developmental Biology

journal homepage: www.elsevier.com/locate/developmentalbiology

Short Communication

The zinc finger protein Zfpm1 modulates ventricular trabeculation through Neuregulin-ErbB signalling

Yuxi Yang, Beibei Li, Xue Zhang, Qinshun Zhao, Xin Lou*

Model Animal Research Centre, Nanjing University, China

ARTICLE INFO

Keywords:
Zfpm1
Heart development
Ventricle trabeculation
Neuregulin-ERBB signalling
Zebrafish

ABSTRACT

Ventricular trabeculation is one essential step for generating a functionally competent ventricular wall, while how the early trabeculae carneae forms and subsequently develops into mature chambers is poorly understood. We found that in zebrafish *zfpm1*$^{-/-}$ juvenile, cardiac function is significantly compromised, with hearts exhibiting deformed trabecular meshwork. To elucidate the mechanisms of Zfpm1 function in cardiac trabeculation, we analyzed *zfpm1* mutant hearts more closely and found that loss of Zfpm1 activity resulted in over-activation of Neuregulin-ErbB signalling and abnormally elevated cardiomyocyte proliferation during cardiac trabeculae growth and modeling stages. These results implicate Zfpm1 plays a pivotal role in coordinating trabeculae patterning and growth.

1. Introduction

Cardiac trabeculae are highly organized muscular structures that form as a result of the projection and expansion of endocardium-lined cardiomyocyte into the ventricular lumen (Moorman and Christoffels, 2003). The trabeculae represent a significant percentage of ventricular mass, serve multiple functions from enhancing ventricular efficiency to increase surface area for nutrition and oxygen uptake (Sedmera et al., 2000). Alterations in cardiac trabeculae development can manifest as a variety of congenital defects. Aberrant reduction in trabeculation is usually associated with hypoplastic ventricular wall, which commonly leads to embryonic heart failure and early embryonic lethality (Connor and Thiagarajan, 2007). In contrast, hypertrabeculation and lack of ventricular wall compaction are closely related to left ventricular non-compaction (LVNC), a genetically heterogeneous disorder (Finsterer et al., 2017).

Cardiac trabeculation is a sophisticated morphogenetic process guided by an interactive regulation of ventricular wall growth and the endocardial-, myocardial- and epicardial-derived signals (Zhang et al., 2013). Genetics studies showed endocardial-derived Neuregulins execute an indispensable function for cardiac trabeculation by signalling to cardiomyocytes through its receptors (ErbB4 and ErbB2) to guide trabecular initiation (Pentassuglia and Sawyer, 2009). In mouse, deletion of Nrg1, Erbb4 or Erbb2 results in the abortion of development of myocardial trabeculae in the heart ventricle (Gassmann et al., 1995; Kramer et al., 1996; Lee et al., 1995). Ventricular trabeculation was abrogated in *nrg2* and *erbb2* mutant zebrafish, which indicates an evolutionarily conserved function of Neuregulin-ErbB signalling in this process (Liu et al., 2010; Rasouli and Stainier, 2017). Beside promoting cardiomyocyte proliferation, Neuregulin-ErbB signalling has also been shown to play an important role in regulating cardiomyocyte migration (delamination) to initiate cardiac trabeculation (Liu et al., 2010). Thus, the Neuregulin-ErbB signalling pathway plays central roles in ventricular chamber development, but the mechanisms underlying transcriptional regulation of key components of this pathway are unresolved.

GATA factors are notable for governing the development of heart, blood cells and other tissues and organs in vertebrates. In most metazoan species have been studied, co-factors termed Friend of GATA (FOG) proteins have been identified that function exclusively with GATA factors and regulate downstream gene expression through a variety of modes (Chlon and Crispino, 2012). Zfpm1 (Zinc Finger Protein, FOG Family Member 1, previous known as FOG1) is a 110 kDa protein with nine zinc finger domains, the C2HC type zinc fingers on Zfpm1 protein are responsible for mediating the interaction with the N-finger of GATA factors (Fox et al., 1999). Zfpm1 also contains two domains that are known to recruit transcriptional regulatory complexes. The one located at the extreme N-terminus is essential to recruit the nucleosome remodeling and histone deacetylase (NuRD)

Abbreviations: dpf, days post fertilization; GFP, green fluorescent protein; HDACs, histone deacetylases; hpf, hours post fertilization; LVNC, left ventricular non-compaction; NuRD, nucleosome remodeling and deacetylase complex; sgRNA, single guide RNA; TEM, transmission electron microscopy; WGA, wheat germ agglutinin; ZFPM, zinc finger protein FOG family member

* Correspondence to: Model Animal Research Centre, Nanjing University, Rm 403B, 12 Xuefu Road, Nanjing, Jiangsu, China.
E-mail address: xin.lou@nju.edu.cn (X. Lou).

https://doi.org/10.1016/j.ydbio.2019.01.001
Received 5 August 2018; Received in revised form 26 December 2018; Accepted 1 January 2019
Available online 03 January 2019

complex, another one between zinc fingers 6 and 7 could bind to CtBP co-repressor (Hong et al., 2005; Katz et al., 2002). Previous studies showed Zfpm1 functions predominantly in the hematopoietic system through interactions with GATA1/2/3 (Amigo et al., 2009; Chang et al., 2002; Sugiyama et al., 2008), but it also has functions in other tissues, including the gonads, intestine and heart (Jacobsen et al., 2005; Katz et al., 2003; Thompson et al., 2005). Knock-down *zfpm1* in zebrafish embryo through morpholino injection led to defects in heart tube looping, anemia and expands myeloid-progenitor cells (Amigo et al., 2009; Walton et al., 2006), while the function of *zfpm1* on cardiac chamber maturation has not been characterized since the limited window of effectiveness for morpholinos.

In the present study, using *zfpm1* knock out zebrafish lines generated with CRISPR-Cas9 technology, we examined the function of *zfpm1* on cardiac chamber maturation. Our results demonstrated that trabecular meshwork in the ventricle of *zfpm1* knock out animal is highly deformed. Transcriptome profiling revealed expression of neuregulin 1 was significantly up-regulated in Zfpm1$^{-/-}$ juvenile, led to over-activation of Neuregulin-ErbB signalling. Our findings also revealed cardiomyocyte proliferation was abnormally enhanced in *zfpm1* knock out juvenile fish, which eventually caused ventricular hypertrabeculation. Thus, Zfpm1 plays an essential role in coordinating zebrafish ventricular trabeculae patterning and growth.

2. Materials and methods

2.1. Ethics approval

The zebrafish used in this study were regularly maintained and handled in accordance with approved guidelines of the Institutional Animal Care and Use Committee of the Nanjing University.

2.2. Zebrafish

Zebrafish embryos were maintained and staged using standard techniques (Westerfield, 2007). Fish lines used were the wild-type Tübingen (TU) strain, Tg(myh7:GFP) and Tg(kdrl:GFP) fish have been previously described (Huang et al., 2003; Jin et al., 2005).

2.3. Generation of knock-out zebrafish line

gRNAs were designed by using CRISPR Design online toolbox (http://crispr.mit.edu). 50 pg of sgRNAs and 500 pg of Cas9 mRNA were co-injected into one-cell stage embryos. The Zfpm1$^{+/\Delta 22}$ allele and zfpm2b$^{+/\Delta 23}$ allele was used for subsequent experiments. Detailed genotyping primers were listed in Table S1.

2.4. Imaging

Whole imaging was performed using a Leica DFC320 camera on a Leica M205FA stereomicroscope. On-section *in situ* hybridization images were captured by using a DS-U3 CCD camera equipped on a Nikon ECLIPSE Ni microscope. All confocal images were acquired using a Zeiss LSM880 confocal microscope. Live images of zebrafish hearts were taken as previously described (Chi et al., 2008).

2.5. Survival Curve

Sixty each WT siblings and Zfpm1$^{-/-}$ were put into 3 L tank from 7 dpf. Every three days, the number of living fish was counted till 60 dpf. Kaplan-Meier curve was generated with Prism 6 (GraphPad) (Goel et al., 2010).

2.6. RNA in situ hybridization

Transcription of DIG-labeled antisense RNA probes was performed using standard methods.

Whole-mount RNA *in situ* hybridization (WISH) was carried out as previously described (Thisse and Thisse, 2008). *In situ* hybridization on cryosections was performed as described previously (Myat et al., 1996; Poss et al., 2002).

2.7. O-Dianisidine staining

Detection of hemoglobin by *o*-dianisidine staining was performed as described (Ransom et al., 1996). Briefly, live embryos were incubated with staining buffer (0.6 mg/mL *o*-dianisidine, 0.01 M sodium acetate, pH 4.5, 0.65% hydrogen peroxide, and 40% ethanol) for 15 min in the dark. Then fixed with 4% paraformaldehyde for 30 min at room temperature. Presence of brown coloration indicates the hemoglobin in red blood cell.

2.8. Masson's trichrome staining and WGA staining

For Masson's trichrome staining, samples were fixed in 4% paraformaldehyde (PFA), then washed, dehydrated in gradient ethanol and plastic embedded. Slides were stained with a modified Masson's trichrome procedure (Sigma Diagnostics Procedure No. HT15), omitting the Bierbich Scarlet-Acid Fuchsin stain. For WGA staining, hearts were fixed in 4% PFA overnight at 4 °C, equilibrated for several hours in 30% sucrose, and embedded with OCT for cryosectioning (14 μm). WGA staining was performed as previously described (Sarmah et al., 2010).

2.9. Transmission Electron Microscopy

Samples were fixed in 2.5% glutaraldehyde in PBS at 4 °C for 48 h, then post-fixed with 1.0% osmium tetroxide. Sample processing and sectioning were carried out as previously described (Hou et al., 2017), imaging was applied with a Hitachi S-7650 transmission electron microscope.

2.10. Measurement of body length and ventricle area to body length

Dissected hearts were imaged with a Leica DFC320 camera on a Leica M205FA. ImageJ was used to calculate the area of the ventricle from these images in pixels squared. The number of pixels per mm was calculated to convert the ventricle area into mm^2. To determine ventricle area to body length, the ventricle area in mm^2 was divided by body length (mm). Body length was manually measured with a millimeter ruler, from the tip of the mouth to the body/caudal fin juncture (Sun et al., 2009).

2.11. Measurement of cardiac function

Red blood cell flow rate in caudal fin was determined as described (Hoage et al., 2012). Briefly, anesthetized zebrafish was placed on a microscope slide in a thin layer of Methyl Cellulose and videos were made with the Nikon NIS-element BR software. Speed was determined in mm/second for a red blood cell to travel between two points.

2.12. Quantification of cell surface, trabecula length and trabecular complexity

For cell surface area quantification, 18 dpf zebrafish cardiomyocytes membrane was labeled with WGA staining. ImageJ software was used to adjust the threshold of cell surface edge and measure cell area individually by ROI manager. Quantification of trabecular complexity was applied as previously described (D'Amato et al., 2016). Briefly, 7 μm plastic sections from dissected 60 dpf wild-type and Zfpm1$^{-/-}$ hearts were stained with Masson's trichrome staining to facilitate visualization of ventricular structures. ImageJ software was used for measurements. The length of trabecula was measured and covert pixels into micrometer. The complexity of trabecular myocardium indicates

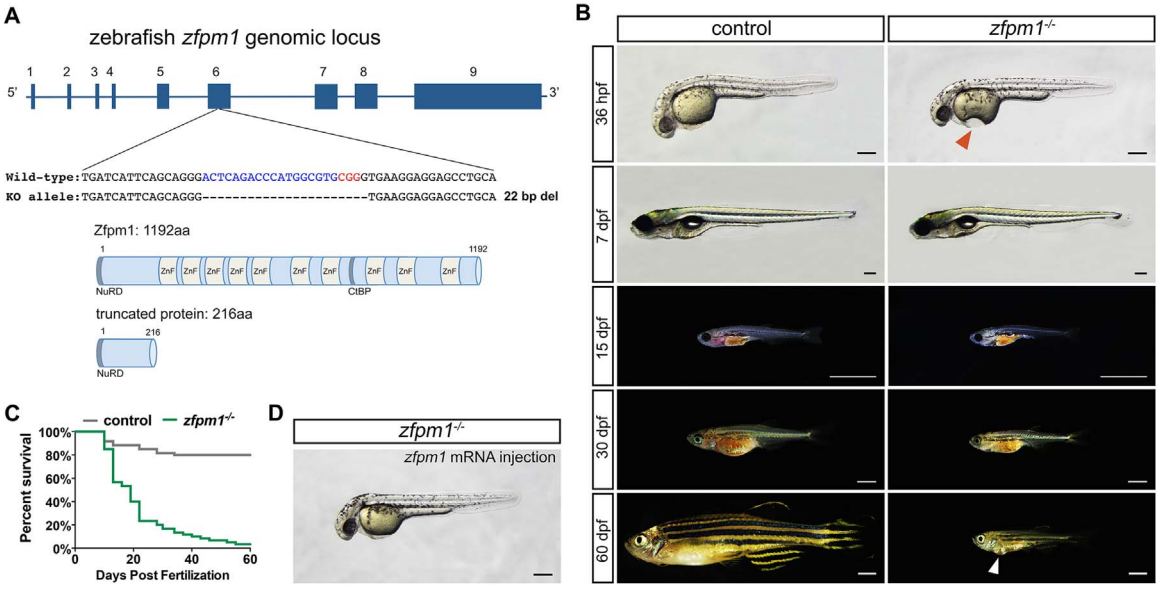

Fig. 1. Generation of Zfpm1 knock out zebrafish line. (A): Upper panel, the zebrafish Zfpm1 genomic locus and Cas9/sgRNA targeting site. Deletions in Δ22 allele are shown as dashes. Lower panel, schematic representations of the domain structure of the wild-type zebrafish Zfpm1 protein and truncated protein derived from the Δ22 allele. (B) Live images of control and Zfpm1$^{-/-}$ zebrafish at designated time points. Lateral view, anterior to the left. Red arrowhead indicates the depression on the yolk of Zfpm1$^{-/-}$ embryo, white arrowhead indicates the bulge on the ventral side of Zfpm1$^{-/-}$ fish. For 36hpf embryos and 7dpf larvae, scale bar: 200 μm. For animal from 15 dpf to 60 dpf, scale bar: 2 mm. (C) Representative Kaplan-Meier plot for Zfpm1$^{-/-}$ fish and clutchmates from one of three independent experiments. 80 total Zfpm1$^{-/-}$ animals and 88 total siblings were followed. P < 0.0001, Mantel-Cox test. (D) Injection of Zfpm1 mRNA rescue the morphological defects in Zfpm1$^{-/-}$ embryos. Scale bar: 200 μm. (For interpretation of the references to color in this figure legend, the reader is referred to the web version of this article.)

the size of the trabecular mesh of myocardial fibers and obtained by dividing the length of each trabecula by its thickness.

2.13. BrdU incorporation assay

BrdU incorporation analysis was performed as previously described (Raya et al., 2003). To quantify BrdU incorporation, the number of BrdU positive nuclei were divided by the total number of cardiomyocyte nuclei counted on sections. Images were processed with ImageJ software.

2.14. RNA-seq analysis and data processing

mRNA from pooled embryos or hearts were extracted and sequenced as previously described (Zhang et al., 2018). Gene differential expression was analyzed by DESeq. 2 (Anders et al., 2015; Love et al., 2014). Genes showing altered expression with adjusted P < 0.05 were considered differentially expressed. The genes with differential expression in Zfpm1 mutants are listed in Table S2 and S4. Heatmap of gene expression was generated by R packages gplots and ggplot2 (Wickham, 2009). Functional annotation of DEG was performed using DAVID (Huang et al., 2008), and a set of enriched GO terms were selected according to relevant criteria related to the biological process studied. R package GOPlot (Walter et al., 2015) was used to generate chord plot to better visualize the relationships between genes and the selected enriched GO terms. The high throughput data generated in this study have been deposited at Gene Expression Omnibus under accession number GSE95118.

2.15. Preparation of cardiomyocyte and endocardial cells

Ventricular cardiomyocyte and endocardial cells were isolated as described previously (Wang et al., 2015). Briefly, ventricles were dissected from control and Zfpm1 mutant animals with Tg(myh7: GFP) or Tg(kdrl1: GFP) transgene at 18 dfp then put on ice and washed several times to remove blood cells. Ventricles were digested in an Eppendorf tube with 0.5 ml HBSS plus 0.13 U ml21 Liberase DH (Roche) and 1% sheep serum at 37 °C while stirring gently with a magnetic stirring bar. Supernatants were collected every 5 min and neutralized with sheep serum. Dissociated cells were spun down and sorted using a BD FACSVantage SE sorter for GFP-positive cells.

2.16. Quantitative real-time PCR

Total RNA was prepared using TRIzol (Invitrogen, Life Technologies Corp.) and Direct-zol™ RNA Miniprep (Zymo Research) from control or Zfpm1 mutant samples. CDNA was synthesized with PrimeScript RT kit (Takara). RT-qPCR reactions were performed on the LightCycler (Roche) system using the SYBR Green Master Mix (Takara). Melt curves were examined to ensure primer specificity. Primers used in RT–qPCR were designed to span exon-exon junctions and were listed in Table S1.

2.17. Western blotting

Proteins from zebrafish hearts were isolated and analyzed as previously described (Zhang et al., 2018). Information for primary antibodies is listed in Table S6.

2.18. Statistics

Statistics were carried out using Prism 7 Software (GraphPad). Survival curve was analyzed with Mantel-Cox tests. Other statistical tests were performed using two-sided, unpaired Student's *t*-tests and where numerical data are presented as mean ± s.e.m. Differences were considered significant if the probability value was $P < 0.05$ and highly significant if the probability value was $P < 0.01$. All experiments were carried out with at least three biological replicates. The numbers of animals used are described in the corresponding figure legends.

3. Results and discussion

3.1. Generation of Zfpm1 knock-out zebrafish

As part of joint efforts to generate knock-out zebrafish line for all annotated transcription regulatory genes and analyze their function in cardiovascular system development, we used CRISPR-Cas9 strategy to disrupt the zebrafish Zfpm1 gene. Multiple sgRNAs targeting Zfpm1 were designed (Fig. 1A and Fig. S1), transcribed and injected into 1-cell stage zebrafish embryo with Cas9 mRNA. F1 individuals were generated by cross the injected founders with wild-type TU fish and screened for presence of insertion or deletion (indel) on Zfpm1 loci. Among the alleles were obtained and displayed consistent phenotype (Fig. S1) through this procedure, the one bearing a 22-bp deletion on 6th exon of Zfpm1 was chosen to be used in the subsequent analysis (Fig. 1A).

To investigate the function of Zfpm1 on development, embryos from multiple Zfpm1$^{+/-}$ incrosses were collected and raised to the adult stage. Prior to 36 hpf, no perceivable morphological difference between Zfpm1$^{-/-}$ embryo and wild-type was observed (data not shown). At 36 hpf, a depression on yolk could be observed on Zfpm1$^{-/-}$ embryo, with slower heart beating and less circulating erythrocytes compare to control siblings (Fig. 1B and Movie S1). Interestingly, the morphological defects and abnormalities on circulation in Zfpm1$^{-/-}$ embryo were gradually recovered, by 7 days post-fertilization (dpf), Zfpm1$^{-/-}$ larvae and wild-type became indistinguishable (Fig. 1B and MovieS2). From 15 dpf, Zfpm1$^{-/-}$ fish exhibited evident growth retardant and substantial mortality (Fig. 1C. 23.3% survival at 22 dpf and 3.3% survival at 60 dpf in Zfpm1$^{-/-}$ fish verse 85.0% and 80.0% in controls; n = 80; P < 0.0001, Mantel-Cox test). Other than growth cessation, Zfpm1$^{-/-}$ fish also displayed notable ventral bulge that indicating dysfunctional and enlarged heart (Fig. 1B).

Supplementary material related to this article can be found online at doi:10.1016/j.ydbio.2019.01.001.

To confirm that loss of Zfpm1 represents the causal event in the phenotypes displayed in our Zfpm1 knock-out line, expression of Zfpm1 was determined and decreased mRNA level was observed in Zfpm1$^{-/-}$ embryos (Fig. S1). Furthermore, mRNA encoding wild-type Zfpm1 was injected into embryos from incrosses of Zfpm1$^{+/-}$ fish and morphological defects in Zfpm1$^{-/-}$ embryos at 36 hpf were efficiently rescued (Fig. 1D).

3.2. Impaired heart development and primitive erythropoiesis in Zfpm1$^{-/-}$ embryos are spontaneously recovered

Previous studies (Amigo et al., 2009; Walton et al., 2006) and preliminary observation from our Zfpm1$^{-/-}$ embryos indicated Zfpm1 participated in early heart development and haematopoiesis, we carried out a set of experiments over an extended time span to further characterize these phenotypes.

By introducing Tg(myh7:GFP) transgene into the Zfpm1 knock out background, we first monitored morphogenesis of heart chambers. Live images from different developmental stages indicated in Zfpm1$^{-/-}$ embryos the heart tube formed normally while the looping of heart chamber was delayed (Fig. S2A). As development process, the morphogenesis of heart was gradually recovered, at 7 dpf, heart of Zfpm1$^{-/-}$ larvae showed normal morphology and ventricle trabeculation normally initiated (Fig. S2A). Development of endocardium and heart valves in Zfpm1$^{-/-}$ embryos were visualized by introducing Tg(kdrl1:

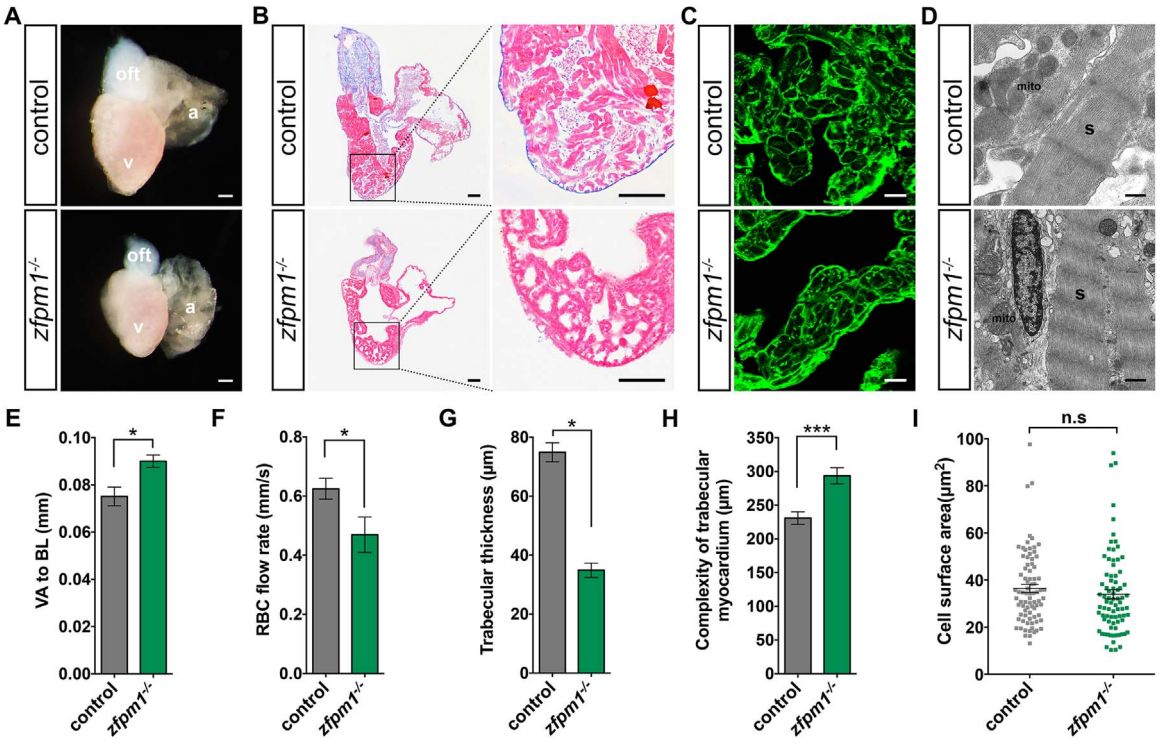

Fig. 2. Loss of Zfpm1 results in cardiac chamber maturation defects. (A) Representative images of dissected hearts from Zfpm1$^{-/-}$ and WT sibling fish at 60 dpf. a, atrium; v, ventricle; oft, outflow tract. Scale bar: 200 μm. (B) Histological analysis of Zfpm1$^{-/-}$ and WT sibling fish. Heart sections were Masson's trichrome stained. Scale bar: 100 μm. (C) Representative images of ventricle sections stained with WGA to indicate cardiomyocyte cell size at 60 dpf. Scale bar: 10 μm. (D) Transmission electron microscopy (TEM) on control and Zfpm1$^{-/-}$ hearts revealed no overt defects on myocardium ultrastructure. s, sarcomere; mito, mitochondrion; Scale bar: 5 μm. (E) Quantification of ventricle area to fish length (VA/BL) index, which was used as a measurement of the cardiomegaly. 10 control fish and 5 Zfpm1$^{-/-}$ fish were examined. (F) Quantification of red blood cell flow rate, which was used as a measurement of the cardiac function. 8 control fish and 7 Zfpm1$^{-/-}$ fish were examined. (G) Quantification of trabecular thickness at 60 dpf. (H) Quantification of the complexity of trabecular myocardium layer at 60 dpf. G to H, 12 sections from 3 wt and 12 sections from 3 Zfpm1$^{-/-}$ fish were examined. E to H, data are mean ± s.e.m. (I) Quantification of cardiomyocyte cell size in control and Zfpm1$^{-/-}$ fish. The surface area of individual cardiomyocyte was plotted. Sections from 3 fish for each genotype were examined. n.s: not significant. * p < 0.05. ** p < 0.01. *** p < 0.001.

GFP) transgene. At 36 hpf, endocardium in Zfpm1$^{-/-}$ embryos displayed severe stenosis (Fig. S2B), which could contribute to the faulty blood circulation phenotype at this stage. From 48 hpf, endocardium in Zfpm1$^{-/-}$ embryos progressively inflated, by 5 dpf, both the superior and inferior valve leaflets were formed in Zfpm1$^{-/-}$ embryos as in wild type (Fig. S2B).

The previous studies showed targeted deletion of Zfpm1 in mouse or knocked down Zfpm1 in zebrafish blocks primitive erythropoiesis at the proerythroblast stage (Amigo et al., 2009; Yao et al., 1998), we confirmed whether Zfpm1 played an evolutionarily conserved function in zebrafish erythropoiesis. O-dianisidine staining results showed loss of Zfpm1 caused a moderate reduction of primitive erythrocyte in Zfpm1$^{-/-}$ embryos at 36 hpf. While similar to the scenarios happened on myocardium and endocardium, impaired erythropoiesis in Zfpm1$^{-/-}$ embryos gradually recovered as development processed (Fig. S2C).

Zfpm1 have been shown to exert its biological function through regulating transcription, in order to determine how mutation of Zfpm1 affects the transcriptome during early zebrafish embryogenesis, we pursued RNA-Seq on wild-type and Zfpm1$^{-/-}$ embryos at 36 hpf. A total of 2059 genes, consisting of 1231 with decreased and 828 with increased expression, were significantly altered in the Zfpm1$^{-/-}$ embryos (fold change (FC) > 1.5, FDR < 0.05) (Table S2). Interestingly, expression of most of cardiovascular development-related genes showed mild or no change in Zfpm1$^{-/-}$ embryos compare to wild-type. We further applied Gene ontology (GO) analysis on genes misregulated in Zfpm1$^{-/-}$ embryos, no GO terms linked to cardiovascular development were enriched (Table S3). To confirmed the RNA-Seq results, whole mount in situ hybridization was applied at 36 hpf to examine the expression of a set of key cardiac regulator gene, including nppa, nkx2.5, tbx5a and gata5. The results confirmed no overt change on expression of these genes in Zfpm1$^{-/-}$ embryos compare to wild type (Fig. S2D).

To better delineate the cardiac phenotype in Zfpm1 KO zebrafish, detailed Zfpm1 expression pattern was analyzed. Whole mount *in situ* hybridization experiments showed Zfpm1 mRNA could be detected in the heart from around 24 hpf (Fig. S3D'). Interestingly, the cardiac expression of Zfpm1 is reduced at 48 hpf and reappeared from 72 hpf (Fig. S3 F', G' and H'). From 12 dpf, the expression of Zfpm1 could be clearly observed in endocardial cells (Fig. S3 I and J). This dynamic, on-off-on pattern matches the timeline of phenotype in Zfpm1 KO animal and suggests Zfpm1 could play stage-specific functions on heart development by regulating gene expression in endocardium.

These data suggested during zebrafish embryogenesis, Zfpm1 played a limited role in embryonic heart development. Since the early abnormalities spontaneously recovered, the Zfpm1$^{-/-}$ juvenile presented an opportunity for investigating the function of Zfpm1 on late developmental events.

3.3. *Zfpm1$^{-/-}$ zebrafish exhibits defected heart chamber maturation*

As development processed, Zfpm1$^{-/-}$ zebrafish exhibited growth retardant and ventral bulge (Fig. 1B), suggesting compromised cardiac function. We euthanized adult Zfpm1$^{-/-}$ zebrafish and assessed the globe morphology of hearts, histological and cell biology features of myocardium.

At 60 dpf, enlarged ventricles (measure by ventricle area to body length index) and dilated atrium were observed in Zfpm1$^{-/-}$ zebrafish, with no overt outflow track or cardiac valves malformation (Fig. 2A and B). Since in fish the ventricle is the cardiac chamber that is principally responsible for pumping blood into arteries, the dilated atrium in Zfpm1$^{-/-}$ zebrafish was likely the secondary phenotype associated with dysfunction of ventricle, we focus following analysis on ventricle.

Histological examination revealed wild-type fish had a thick ventricular wall and well-grown trabeculae, whereas Zfpm1$^{-/-}$ zebrafish exhibited substantial thinner trabeculae and anomalous spongy trabeculae network with significantly higher complexity (Fig. 2B, G, and H). By measuring the speed of red blood cell flow, cardiac function of Zfpm1 KO was analyzed. The results showed slower flow speed compare to control animal (Fig. 2F) and this result indicated the cardiac function was compromised in Zfpm1$^{-/-}$ zebrafish.

To explore whether this phenotype is caused by defected cardiomyocyte differentiation, cell morphology of cardiomyocyte and cardiac sarcomere assembling was examined. WGA staining showed cardiomyocyte in Zfpm1$^{-/-}$ zebrafish displayed relative normal morphology and the cell surface area is comparable to wild-type (Fig. 2C and I), transmission electron microscopy also revealed no overt abnormality on cardiac sarcomere in Zfpm1$^{-/-}$ zebrafish (Fig. 2D). These results indicated the spongy-like trabeculae could be caused by hypertrabeculation.

As development process, the ventricle compensates for increasing hemodynamic demands by developing a thickened wall of muscle and generating a complex network of trabeculae carneae. The process of ventricular chamber maturation involves the intricate spatiotemporal regulation of cardiomyocyte proliferation and migration (Foglia and Poss, 2016). We examined ventricle maturation in Zfpm1$^{-/-}$ juvenile to determine the time point Zfpm1 exerted its function in this process. Prior to 12 dpf, the morphology of ventricle and development of trabeculae carneae in Zfpm1$^{-/-}$ juvenile are comparable to control juvenile (Fig. 3A). From 12 dfp, a significantly higher number of trabeculae could be observed in ventricles from the Zfpm1$^{-/-}$ juvenile (Fig. 3B). At 15 dpf, ventricles in the Zfpm1$^{-/-}$ juvenile are slightly

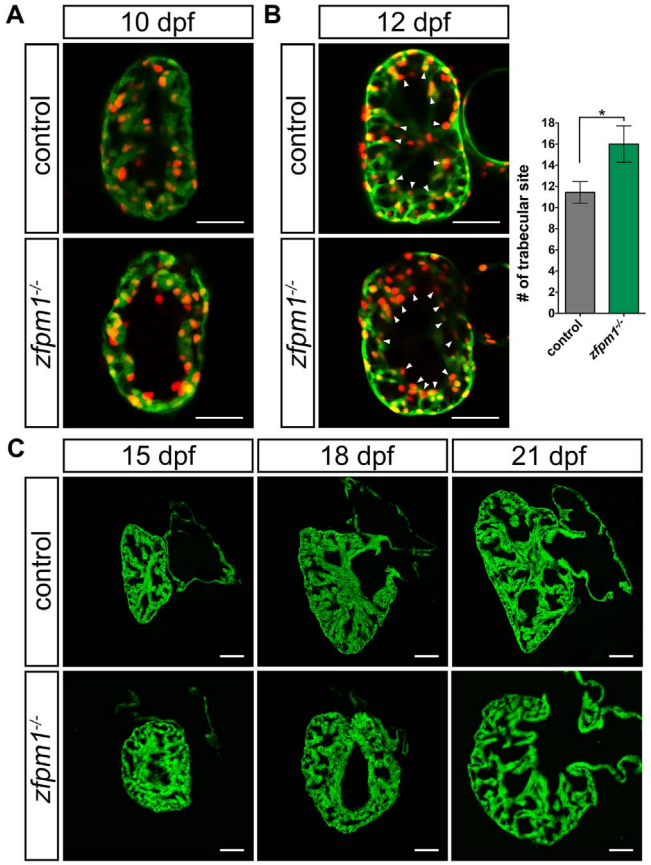

Fig. 3. Loss of Zfpm1 led to trabeculation deformation in ventricle. (A) Confocal images (mid-sagittal optical sections) of larval hearts from control and Zfpm1$^{-/-}$ animals at 10 dpf. (B) Left panels, confocal images (mid-sagittal optical sections) of larval hearts from control and Zfpm1$^{-/-}$ animals at 12 dpf. Arrowheads indicated sites where trabecular is initiating. Right panel, quantification of number trabecular initiation site on section. 8 sections from control and 12 sections from Zfpm1$^{-/-}$ fish were examined. Data are mean ± s.e.m. * $p < 0.05$. A and B, cardiomyocyte was labeled with Tg(myh7: GFP; myh7: DsRed-Nuc) transgenes. (C) Confocal projections of zebrafish juvenile hearts section at designated time points showing the abnormal trabeculation in Zfpm1$^{-/-}$ animals. Cardiomyocyte was labeled with Tg(myh7: GFP) transgene. Scale bars, 50 μm.

enlarged compared with the control, trabeculae carneae in Zfpm1$^{-/-}$ juvenile is shorter which leading to the formation of a cavity (Fig. 3C). At 18 dpf, ventricles in the Zfpm1$^{-/-}$ juvenile displayed a rounder morphology compare with the control, trabeculae carneae is notably thinner in the Zfpm1$^{-/-}$ juvenile and started showing a spongy-like organization (Fig. 3C). By 21 dpf, a large ventricle cavity was formed and the ventricles become more dilated in Zfpm1$^{-/-}$ juvenile compare with the control (Fig. 3C). This data indicated Zfpm1 plays an important role in modulating the maturation of ventricle, especially on the patterning and growth of trabeculae carneae.

The zebrafish genome has two homologs of Zfpm1: zfpm2a and zfpm2b, the protein product of both genes has a high degree of conservation in the domain arrangement compare to Zfpm1 (Chlon and Crispino, 2012) and expressed in the heart during zebrafish embryo development (Fig. S3A and data not shown). To systematically investigate the function of Zfmp proteins on vertebrate development, we examined zfpm2a$^{-/-}$ and zfpm2b$^{-/-}$ embryos. The zfpm2a gene-trapping line was derived from a tol2 transposase based gene-trapping screen (Hou et al., 2017) and the zfpm2b knock outline was generated through CRISPR-Cas9 technology (Fig. S3 A and B). Neither zfpm2a$^{-/-}$ or zfpm2b$^{-/-}$ embryos displayed detectable defects in cardiovascular system development and erythropoiesis, furthermore, zfpm2a$^{-/-}$ and zfpm2b$^{-/-}$ animal exhibited normal growth and mortality compared to wild-type siblings (data not shown). On the basis of likelihood of redundancy as gleaned from the zfpm2a and zfpm2b expression data, double mutants were generated. The zfpm2a; zfpm2b double knock out animals displayed normal embryogenesis (Fig. S3C), while as development processed, severer growth cessation emerged from around 30 dpf (Fig. S3D). Globe morphology of hearts from adult zfpm2a; zfpm2b double knock out fish was normal and histological examination revealed no overt defects on cardiac chamber maturation (Fig. S3D). These results indicated in zebrafish, zfpm2a and zfpm2b are dispensable for ventricle maturation.

3.4. Zfpm1 modulates Neuregulin-ErbB signalling during ventricular maturation

As a dedicated co-factor of GATA family transcriptional regulators, Zfpm1 can both facilitate and antagonize GATA factor transcriptional regulation depending on the context (Chlon and Crispino, 2012). In order to determine how loss of Zfpm1 affects transcriptome during cardiac chambers maturation, we pursued RNA-Seq on ventricles from

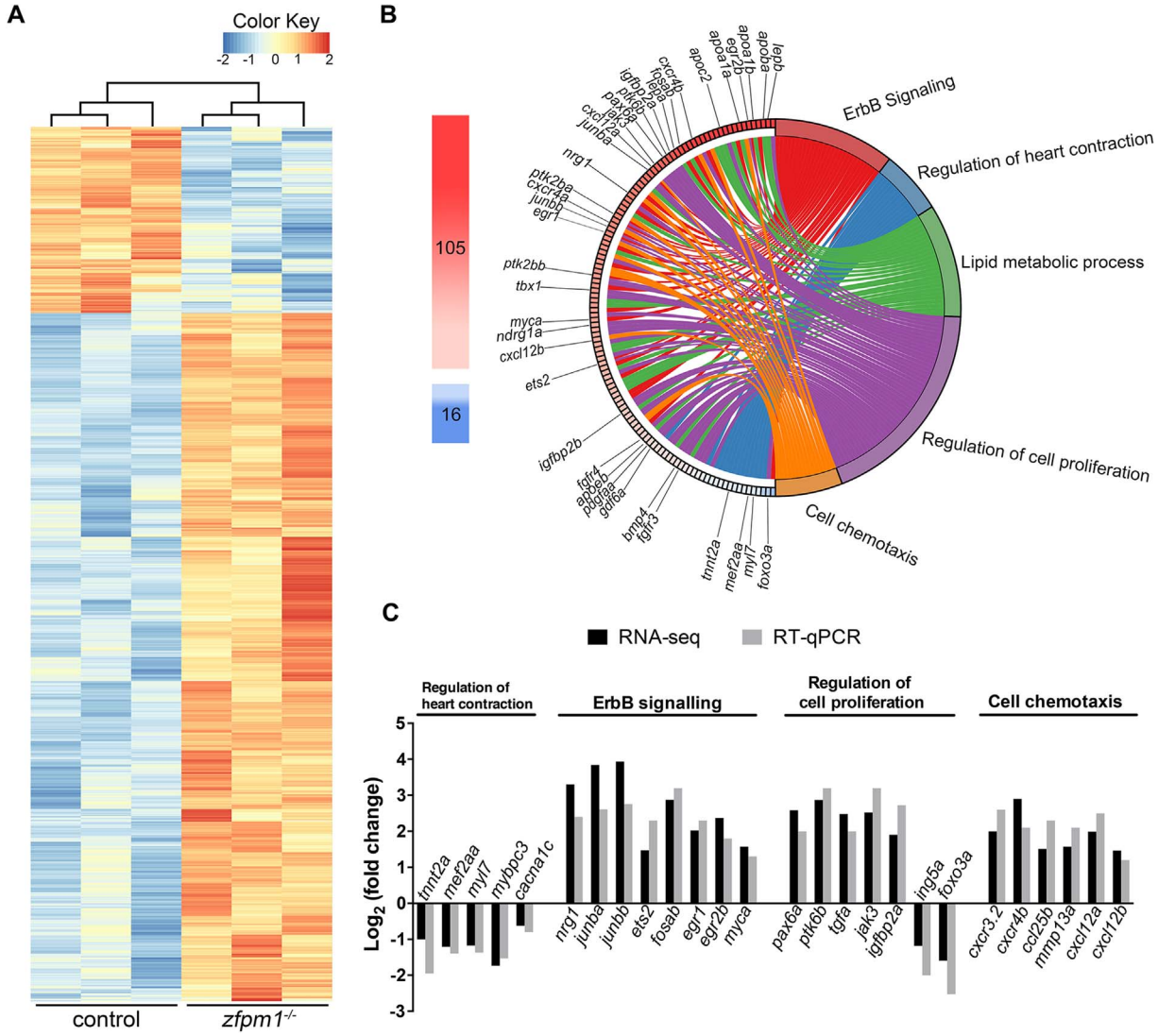

Fig. 4. Gene expression profiling of Zfpm1$^{-/-}$ ventricles. (A) Heat map representation of genes differentially expressed in Zfpm1$^{-/-}$ ventricles at 21 dpf. Red, upregulated; blue, downregulated; white, no significant change. (B) Circular plot of 121 representative differentially expressed genes, simultaneously presenting a detailed view of the relationships between expression changes (left semicircle perimeter) and processes (right semicircle perimeter). 47 of the 121 genes are named. Red, upregulated; blue, downregulated. Code color means the $\log_2$(fold change) value. Details in Supplementary Table S4 and S5. (C) Comparison of the changes in expression of selected genes measured by RNA-seq and RT–qPCR. (For interpretation of the references to color in this figure legend, the reader is referred to the web version of this article.)

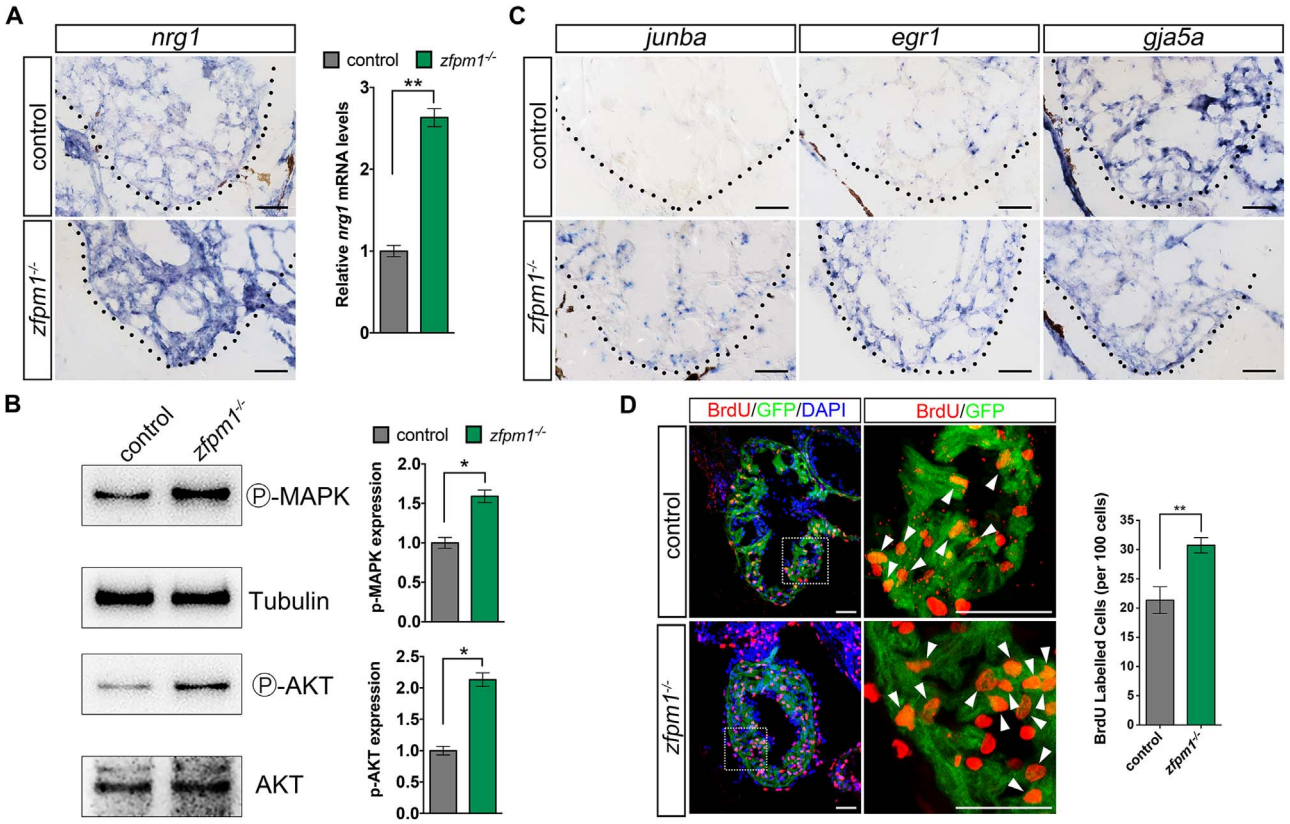

Fig. 5. Loss of Zfpm1 led to the elevation of Neuregulin-ErbB signalling activity and transit enhanced cardiomyocytes proliferation. (A) Left panel, *in situ* hybridization for nrg1 on ventricle sections from 18 days old control and Zfpm1 mutant animals. Right panel, qPCR experiments confirmed up-regulation of nrg1 in endocardial cell. Error bars represent mean ± SEM. ** $p < 0.01$. (B) Left panel, representative Western blot demonstrating elevated phosphor-MAPK and phosphor-AKT level in hearts of Zfpm1 mutant animals. Tubulin and total AKT were used as loading control. Left panel, quantification of phosphor-MAPK and phosphor-AKT proteins normalized by either Tublin or total AKT. Error bars represent mean ± SEM. * $p < 0.05$. (C) *In situ* hybridization for Neuregulin-ErbB signalling target genes on ventricle sections from 18 days old control and Zfpm1 mutant animals. (D) Ventricles from 18 days old control and Zfpm1 mutant animals stained for BrdU incorporation (red) to assess cardiomyocyte proliferation. Middle panels, high-magnification images of the boxed areas in the left panels. Arrowheads indicated the proliferating cardiomyocytes. Scale bar: 50 μm. Right panel, quantification of BrdU-positive nuclei in Zfpm1$^{-/-}$ ventricle, data are mean ± s.e.m. Tg(myh7: GFP) transgene was introduced to identify cardiomyocyte. 8 sections from 4 control and 8 sections from 3 Zfpm1$^{-/-}$ fish were examined. ** $p < 0.01$. (For interpretation of the references to color in this figure legend, the reader is referred to the web version of this article.)

wild-type and Zfpm1$^{-/-}$ juvenile at 18 dpf. A total of 1250 genes, consisting of 266 with decreased and 984 with increased expression, were significantly altered in the ventricles from Zfpm1$^{-/-}$ juvenile (fold change (FC) > 2, FDR < 0.05) (Fig. 4A and Table S4). Majority of the aberrantly expressed genes were up-regulated rather than down-regulated in the ventricles from Zfpm1$^{-/-}$ animal, this result is consistent with models in which Zfpm1 primarily acts as a repressor of transcription. Gene ontology (GO) enrichment analysis revealed genes deregulated in Zfpm1$^{-/-}$ juvenile ventricles involved in the Neuregulin-ErbB signalling pathway, cell cycle and proliferation, regulation of heart contraction, cell chemotaxis and lipid metabolic process (Fig. 4B and Supplementary Table S5). Furthermore, quantitative real-time PCR of the 26 representative genes was applied to support the reliability of expression data obtained by RNA-Seq (Fig. 4C).

Neuregulin-ErbB signalling has been found playing crucial roles in ventricle maturation from patterning trabecular to regulating cardiomyocyte proliferation (Pentassuglia and Sawyer, 2009; Zhang et al., 2013). Based on results from RNA-Seq, we further examined the activity of Neuregulin-ErbB signalling and trabeculae growth in Zfpm1$^{-/-}$ juvenile. On-section *in situ* hybridization confirmed the cardiac expression of *nrg1* was significantly up-regulated (Fig. 5A). To further confirm the source of nrg1, q-PCR was applied on endocardial cells prepared from control and Zfpm1$^{-/-}$ juvenile by FACS. The results showed enhanced nrg1 expression in endocardial cell from Zfpm1$^{-/-}$ samples (Fig. 5A). This indicated Zfpm1majorly executes its function on nrg1 transcription regulation in endocardial cell. To examine whether upregulation in nrg1 expression could lead to enhancement of ErbB signalling, the phosphorylation level of MAPK and AKT were examined and increased phosphorylation of both proteins in Zfpm1$^{-/-}$ samples was observed (Fig. 5B). The expression of targets gene, junba, erg1 and erg2b (Fromm and Rhode, 2004; Sweeney et al., 2001), was explored and the stronger signal in Zfpm1$^{-/-}$ samples further confirmed arisen Neuregulin-ErbB signalling activity (Fig. 5C and data not shown). Other trabecular markers, including gja5a, also displayed disarrayed expression in Zfpm1$^{-/-}$ ventricles (Fig. 5C and data not shown). Recently, researchers found trabeculation appears unaffected in nrg1 mutant while nrg2a is required for cardiac trabeculation in zebrafish (Rasouli and Stainier, 2017; Samsa et al., 2016). Interestingly, RNA-seq and qPCR results showed the expression of nrg2a and nrg2b have not altered in Zfpm1$^{-/-}$ ventricles (data not shown). Analysis of BrdU incorporation revealed increased proliferation (8–10%) of trabecular cardiomyocytes in the hearts of Zfpm1$^{-/-}$ juvenile (Fig. 5D). Elevated cardiomyocyte proliferation reflected excessive initiation of trabeculae which could contribute to the high complexity of trabeculae observed on later stages. These results indicated Zfpm1 modulates Neuregulin-ErbB signalling activity during zebrafish cardiac chamber maturation.

4. Summary

Here we report genetic functional analysis of the zinc finger protein Zfpm1. Our experiments indicate that during ventricle chamber development, Zfpm1 is an indispensable factor for regulating the

patterning of trabeculation. Loss of Zfpm1 in zebrafish leads to up-regulation of nrg1 expression in developing ventricle and elevates Neuregulin-ErbB activity, leading to abnormal enhanced cardiomyocyte proliferation and improper trabeculae formation. This work provides new insight into the function of Zfpm1 in heart development and suggests a possible role for Zfpm1 in congenital cardiac trabeculae defects.

Acknowledgments

We thank members of Xingxu Huang lab at ShanghaiTech University for helping on the generation of Zfpm1 knock out fish; Qi Xiao at Nanjing University for discussion and drawing the graphical abstract; members of Ian Scott lab at University of Toronto and members of Di Chen lab at Nanjing University for help during this project. This research was undertaken, in part, thanks to grant funding from National Natural Science Foundation of China (NSFC 31671505 and NSFC 31471354 to X.L).

Ethics approval

Zebrafish were housed and handled as per Nanjing University Laboratory Animal Services guidelines. All the protocols involving the use of animals were in accordance with approved guidelines of the Institutional Animal Care and Use Committee of the Nanjing University.

Author contributions

X.L and Q.Z. conceptualized and supervised the project. X.L acquired funding for the project. Y.Y, B.L., and X.Z. performed experiments, analyzed and curated the data. X.L. wrote the original draft and edited the revised manuscript.

Appendix A. Supporting information

Supplementary data associated with this article can be found in the online version at doi:10.1016/j.ydbio.2019.01.001.

References

Amigo, J.D., Ackermann, G.E., Cope, J.J., Yu, M., Cooney, J.D., Ma, D., Langer, N.B., Shafizadeh, E., Shaw, G.C., Horsely, W., Trede, N.S., Davidson, A.J., Barut, B.A., Zhou, Y., Wojiski, S.A., Traver, D., Moran, T.B., Kourkoulis, G., Hsu, K., Kanki, J.P., Shah, D.I., Lin, H.F., Handin, R.I., Cantor, A.B., Paw, B.H., 2009. The role and regulation of friend of GATA-1 (FOG-1) during blood development in the zebrafish. Blood 114, 4654–4663.

Anders, S., Pyl, P.T., Huber, W., 2015. HTSeq–a python framework to work with high-throughput sequencing data. Bioinformatics 31, 166–169.

Chang, A.N., Cantor, A.B., Fujiwara, Y., Lodish, M.B., Droho, S., Crispino, J.D., Orkin, S.H., 2002. GATA-factor dependence of the multitype zinc-finger protein FOG-1 for its essential role in megakaryopoiesis. Proc. Natl. Acad. Sci. USA 99, 9237–9242.

Chi, N.C., Shaw, R.M., Jungblut, B., Huisken, J., Ferrer, T., Arnaout, R., Scott, I., Beis, D., Xiao, T., Baier, H., Jan, L.Y., Tristani-Firouzi, M., Stainier, D.Y., 2008. Genetic and physiologic dissection of the vertebrate cardiac conduction system. PLoS Biol. 6, e109.

Chlon, T.M., Crispino, J.D., 2012. Combinatorial regulation of tissue specification by GATA and FOG factors. Development 139, 3905–3916.

Connor, J.A., Thiagarajan, R., 2007. Hypoplastic left heart syndrome. Orphanet J. Rare Dis. 2, 23.

D'Amato, G., Luxan, G., del Monte-Nieto, G., Martinez-Poveda, B., Torroja, C., Walter, W., Bochter, M.S., Benedito, R., Cole, S., Martinez, F., Hadjantonakis, A.K., Uemura, A., Jimenez-Borreguero, L.J., de la Pompa, J.L., 2016. Sequential Notch activation regulates ventricular chamber development. Nat. Cell Biol. 18, 7–20.

Finsterer, J., Stollberger, C., Towbin, J.A., 2017. Left ventricular noncompaction cardiomyopathy: cardiac, neuromuscular, and genetic factors. Nat. Rev. Cardiol. 14, 224–237.

Foglia, M.J., Poss, K.D., 2016. Building and re-building the heart by cardiomyocyte proliferation. Development 143, 729–740.

Fox, A.H., Liew, C., Holmes, M., Kowalski, K., Mackay, J., Crossley, M., 1999. Transcriptional cofactors of the FOG family interact with GATA proteins by means of multiple zinc fingers. EMBO J. 18, 2812–2822.

Fromm, L., Rhode, M., 2004. Neuregulin-1 induces expression of Egr-1 and activates acetylcholine receptor transcription through an Egr-1-binding site. J. Mol. Biol. 339, 483–494.

Gassmann, M., Casagranda, F., Orioli, D., Simon, H., Lai, C., Klein, R., Lemke, G., 1995. Aberrant neural and cardiac development in mice lacking the ErbB4 neuregulin receptor. Nature 378, 390–394.

Goel, M.K., Khanna, P., Kishore, J., 2010. Understanding survival analysis: Kaplan-Meier estimate. Int. J. Ayurveda Res. 1, 274–278.

Hoage, T., Ding, Y., Xu, X., 2012. Quantifying cardiac functions in embryonic and adult zebrafish. Methods Mol. Biol. 843, 11–20, (Clifton, N. J.).

Hong, W., Nakazawa, M., Chen, Y.Y., Kori, R., Vakoc, C.R., Rakowski, C., Blobel, G.A., 2005. FOG-1 recruits the NuRD repressor complex to mediate transcriptional repression by GATA-1. EMBO J. 24, 2367–2378.

Hou, N., Yang, Y., Scott, I.C., Lou, X., 2017. The Sec domain protein Scfd1 facilitates trafficking of ECM components during chondrogenesis. Dev. Biol. 421, 8–15.

Huang, C.J., Tu, C.T., Hsiao, C.D., Hsieh, F.J., Tsai, H.J., 2003. Germ-line transmission of a myocardium-specific GFP transgene reveals critical regulatory elements in the cardiac myosin light chain 2 promoter of zebrafish. Dev. Dyn. 228, 30–40.

Huang, D.W., Sherman, B.T., Lempicki, R.A., 2008. Systematic and integrative analysis of large gene lists using DAVID bioinformatics resources. Nat. Protoc. 4, 44.

Jacobsen, C.M., Mannisto, S., Porter-Tinge, S., Genova, E., Parviainen, H., Heikinheimo, M., Adameyko, I.I., Tevosian, S.G., Wilson, D.B., 2005. GATA-4: fog interactions regulate gastric epithelial development in the mouse. Dev. Dyn. Off. Publ. Am. Assoc. Anat. 234, 355–362.

Jin, S.W., Beis, D., Mitchell, T., Chen, J.N., Stainier, D.Y., 2005. Cellular and molecular analyses of vascular tube and lumen formation in zebrafish. Development 132, 5199–5209.

Katz, S.G., Cantor, A.B., Orkin, S.H., 2002. Interaction between FOG-1 and the corepressor C-terminal binding protein is dispensable for normal erythropoiesis in vivo. Mol. Cell Biol. 22, 3121–3128.

Katz, S.G., Williams, A., Yang, J., Fujiwara, Y., Tsang, A.P., Epstein, J.A., Orkin, S.H., 2003. Endothelial lineage-mediated loss of the GATA cofactor Friend of GATA 1 impairs cardiac development. Proc. Natl. Acad. Sci. USA 100, 14030–14035.

Kramer, R., Bucay, N., Kane, D.J., Martin, L.E., Tarpley, J.E., Theill, L.E., 1996. Neuregulins with an Ig-like domain are essential for mouse myocardial and neuronal development. Proc. Natl. Acad. Sci. USA 93, 4833–4838.

Lee, K.F., Simon, H., Chen, H., Bates, B., Hung, M.C., Hauser, C., 1995. Requirement for neuregulin receptor erbB2 in neural and cardiac development. Nature 378, 394–398.

Liu, J., Bressan, M., Hassel, D., Huisken, J., Staudt, D., Kikuchi, K., Poss, K.D., Mikawa, T., Stainier, D.Y.R., 2010. A dual role for ErbB2 signaling in cardiac trabeculation. Development 137, 3867–3875.

Love, M.I., Huber, W., Anders, S., 2014. Moderated estimation of fold change and dispersion for RNA-seq data with DESeq. 2. Genome Biol. 15, 550.

Moorman, A.F., Christoffels, V.M., 2003. Cardiac chamber formation: development, genes, and evolution. Physiol. Rev. 83, 1223–1267.

Myat, A., Henrique, D., Ish-Horowicz, D., Lewis, J., 1996. A chick homologue of Serrate and its relationship with Notch and Delta homologues during central neurogenesis. Dev. Biol. 174, 233–247.

Pentassuglia, L., Sawyer, D.B., 2009. The role of neuregulin 1β/ErbB signaling in the heart. Exp. Cell Res. 315, 627–637.

Poss, K.D., Wilson, L.G., Keating, M.T., 2002. Heart regeneration in zebrafish. Science 298, 2188–2190.

Ransom, D.G., Haffter, P., Odenthal, J., Brownlie, A., Vogelsang, E., Kelsh, R.N., Brand, M., van Eeden, F.J., Furutani-Seiki, M., Granato, M., Hammerschmidt, M., Heisenberg, C.P., Jiang, Y.J., Kane, D.A., Mullins, M.C., Nusslein-Volhard, C., 1996. Characterization of zebrafish mutants with defects in embryonic hematopoiesis. Development 123, 311–319.

Rasouli, S.J., Stainier, D.Y.R., 2017. Regulation of cardiomyocyte behavior in zebrafish trabeculation by Neuregulin 2a signaling. Nat. Commun. 8, 15281.

Raya, A., Koth, C.M., Buscher, D., Kawakami, Y., Itoh, T., Raya, R.M., Sternik, G., Tsai, H.J., Rodriguez-Esteban, C., Izpisua-Belmonte, J.C., 2003. Activation of notch signaling pathway precedes heart regeneration in zebrafish. Proc. Natl. Acad. Sci. USA 100 (Suppl 1), 11889–11895.

Samsa, L.A., Ito, C.E., Brown, D.R., Qian, L., Liu, J., 2016. IgG-containing isoforms of neuregulin-1 are dispensable for cardiac trabeculation in zebrafish. PLoS One 11, e0166734.

Sarmah, S., Barrallo-Gimeno, A., Melville, D.B., Topczewski, J., Solnica-Krezel, L., Knapik, E.W., 2010. Sec24D-dependent transport of extracellular matrix proteins is required for zebrafish skeletal morphogenesis. PLoS One 5, e10367.

Sedmera, D., Pexieder, T., Vuillemin, M., Thompson, R.P., Anderson, R.H., 2000. Developmental patterning of the myocardium. Anat. Rec. 258, 319–337.

Sugiyama, D., Tanaka, M., Kitajima, K., Zheng, J., Yen, H., Murotani, T., Yamatodani, A., Nakano, T., 2008. Differential context-dependent effects of friend of GATA-1 (FOG-1) on mast-cell development and differentiation. Blood 111, 1924–1932.

Sun, X., Hoage, T., Bai, P., Ding, Y., Chen, Z., Zhang, R., Huang, W., Jahangir, A., Paw, B., Li, Y.G., Xu, X., 2009. Cardiac hypertrophy involves both myocyte hypertrophy and hyperplasia in anemic zebrafish. PLoS One 4, e6596.

Sweeney, C., Fambrough, D., Huard, C., Diamonti, A.J., Lander, E.S., Cantley, L.C., Carraway, K.L., 3rd, 2001. Growth factor-specific signaling pathway stimulation and gene expression mediated by ErbB receptors. J. Biol. Chem. 276, 22685–22698.

Thisse, C., Thisse, B., 2008. High-resolution in situ hybridization to whole-mount zebrafish embryos. Nat. Protoc. 3, 59–69.

Thompson, B.E., Bernstein, D.S., Bachorik, J.L., Petcherski, A.G., Wickens, M., Kimble, J., 2005. Dose-dependent control of proliferation and sperm specification by FOG-1/CPEB. Development 132, 3471–3481.

Walter, W., Sanchez-Cabo, F., Ricote, M., 2015. GOplot: an R package for visually combining expression data with functional analysis. Bioinformatics 31, 2912–2914.

Walton, R.Z., Bruce, A.E., Olivey, H.E., Najib, K., Johnson, V., Earley, J.U., Ho, R.K., Svensson, E.C., 2006. Fog1 is required for cardiac looping in zebrafish. Dev. Biol. 289, 482–493.

Wang, J., Cao, J., Dickson, A.L., Poss, K.D., 2015. Epicardial regeneration is guided by cardiac outflow tract and Hedgehog signalling. Nature 522, 226–230.

Westerfield, M., 2007. The zebrafish book. A guide for the laboratory use of zebrafish (Danio rerio)Zebrafish International Resource Center 5th ed. University of Oregon Press, Oregon.

Wickham, H., 2009. ggplot2: Elegant Graphics for Data Analysis. Springer Publishing Company, Incorporated, Wickham, Hadley. http://dx.doi.org/10.1007/978-0-387-98141-3, ISBN: 0387981403 9780387981406.

Yao, T.P., Oh, S.P., Fuchs, M., Zhou, N.D., Ch'ng, L.E., Newsome, D., Bronson, R.T., Li, E., Livingston, D.M., Eckner, R., 1998. Gene dosage-dependent embryonic development and proliferation defects in mice lacking the transcriptional integrator p300. Cell 93, 361–372.

Zhang, L., Yang, Y., Li, B., Scott, I.C., Lou, X., 2018. The DEAD-box RNA helicase Ddx39ab is essential for myocyte and lens development in zebrafish. Development 145.

Zhang, W., Chen, H., Qu, X., Chang, C.P., Shou, W., 2013. Molecular mechanism of ventricular trabeculation/compaction and the pathogenesis of the left ventricular noncompaction cardiomyopathy (LVNC). Am. J. Med. Genet. Part C Semin. Med. Genet. 163c, 144–156.